Combustion and Flame 262 (2024) 113338

Contents lists available at ScienceDirect

Combustion and Flame

journal homepage: www.sciencedirect.com/journal/combustion-and-flame

Finding a common ground for RCM experiments. Part B: Benchmark study on ethanol ignition

R.D. Büttgen [a], M. Preußker [a], D. Kang [b], S. Cheng [b], S.S. Goldsborough [b], G. Issayev [c], A. Farooq [c], H. Song [d,1], Y. Fenard [d], G. Vanhove [d], A. Abd El-Sabor Mohamed [e], H.J. Curran [e], K.A. Heufer [a,*]

[a] Chair of High Pressure Gas Dynamics, Shock Wave Laboratory, RWTH Aachen University, Aachen 52056, Germany
[b] Transportation and Power Systems Division, Argonne National Laboratory, Lemont, IL 60439, USA
[c] Clean Combustion Research Center, Physical Sciences and Engineering Division, King Abdullah University of Science and Technology (KAUST), Thuwal 23955, Saudi Arabia
[d] Physicochimie des Processus de Combustion et de l'Atmosphère, University of Lille, CNRS, UMR 8522 - PC2A, Lille F-59000, France
[e] Combustion Chemistry Centre, School of Biological and Chemical Sciences, Ryan Institute, MaREI, University of Galway, Galway, Ireland

ARTICLE INFO

Keywords:
Rapid compression machine
Ethanol
Facility effects

ABSTRACT

Rapid compression machines (RCMs) are widely used to investigate gas phase reaction kinetics of various kind of fuels at application relevant conditions. In principle, the operation of an RCM is based on the idea of compressing a homogenous pre-mixed fuel-air mixture by a piston. Usually creviced pistons ensure a homogenous adiabatic core in the center of the reaction chamber which permits the assumption of an isentropic relation between the measured pressure and gas temperature. Despite the ideal core gas compression, non-ideal effects such as heat loss, differences in the compression behavior, and ultimately non-standardized design and operation of rapid compression machines lead to different experimental results in different facilities at nominally the same end of compression conditions.

In this study ignition delay times of ethanol are investigated at four different conditions in five independent RCMs. As expected, the raw results of the different facilities indeed show notable differences at the same end of compression conditions. However, according to the adiabatic core hypothesis the agreement between kinetic simulations and experiments should be consistent for all facilities provided that the facility effects are correctly accounted for. To elaborate upon this hypothesis, a kinetic mechanism is optimized to reflect the experimental results of all facilities. In the end, the optimized mechanism predicts all experimental data within the expected uncertainty. This confirms the reliability of RCM experiments for kinetic investigations and the validity of the effective volume approach in simulating RCM data.

1. Introduction

Rapid compression machines (RCMs) are widely adopted instruments to investigate the gas phase reaction kinetics of combustion processes [1,2]. Autoignition phenomena are typically investigated by measuring ignition delay times (IDTs) as a function of compressed pressure (p_C), compressed temperature (T_C), initial dilution (O_2 / bath gas) and initial stoichiometry (ϕ) [1,2]. These parameters are chosen to match the thermodynamic conditions of real combustors as e.g., internal combustion engines and/or gas turbines. A comprehensive overview of RCM operation is discussed in the review by Goldsborough et al. [2] and only the main aspects will be discussed here.

In principle, an experiment in an RCM is conducted by compressing a homogeneously premixed gaseous mixture, resulting in increased temperature and pressure, eventually triggering auto-ignition. In contrast to an internal combustion engine (ICE), only a single compression stroke takes place leaving the piston fixed at the end of compression (EOC) position, thus resulting in a constant volume reactor.

A crucial aspect in RCM experiments is that the majority of the compressed gas, referred to as the core gas, can be assumed to be compressed isentropically as described in the adiabatic core hypothesis [2–4]. This is valid as long as non-ideal effects, such as heat loss and

* Corresponding author.
E-mail address: heufer@hgd.rwth-aachen.de (K.A. Heufer).
[1] Current affiliation: Department of Mechanical Engineering, Kumoh National Institute of Technology, 61 Daehak-ro, Gumi-si, Gyeongsangbuk-do, 39,177 Korea.

https://doi.org/10.1016/j.combustflame.2024.113338
Received 16 August 2023; Received in revised form 19 January 2024; Accepted 21 January 2024
Available online 3 February 2024

vortices, are limited to the areas close to the wall. To ensure this, creviced piston designs are utilized in modern RCMs as first suggested by Lee and Hochgreb [5] and further described by Sung and Curran [3]. With a creviced piston a homogenous compressed core gas region can be maintained by capturing the boundary layer during compression and therefore supresses the otherwise induced roll-up vortex. This provides reaction measuring times of up to 150 ms after EOC [2,3]. The adiabatic core hypothesis also permits the deduction of the compressed gas temperature T_C from the measured compressed pressure p_C, the initial pressure p_i, the initial temperature T_i and the mixtures' heat capacity. In this way RCMs can provide an environment with known boundary conditions for chemical kinetic investigations [1–3]. In addition, numerous publications [3,6,7] have shown a high degree of repeatability of individual experiments with regards to the pressure-time history and the resulting chemical kinetic IDTs. This is important because, on the one hand it allows chemical kinetic reactivities to be studied as a function of repeatable and well-known thermodynamic states [2]. Moreover, due to precise repeatability, so-called non-reactive experiments can be carried out, which allows for accurate simulation of the experiments, referred to as the "effective volume approach" discussed in the literature [8,9].

However, experiments conducted in different RCMs at seemingly the same experimental conditions (ϕ, dilution, p_C and T_C) can result in quantitatively different IDTs, as described in the literature [2,10–13]. This lack of direct comparability is not ideal, as no immediate verification or falsification of new experimental data is possible. One reason for this supposed discrepancy of experimental results is generally explained by so-called "facility effects" [1,2,14] in which the heat loss is the most prominent. While the core gas can be assumed to be compressed isentropically, the gaseous boundary layers will lose heat to the colder walls, resulting in an effective volume increase of the adiabatic core, which in turn leads to a reduction in the observed pressure.

This heat loss is not only present after the end of compression where an apparent pressure drop with time can be observed but also during the compression phase. This alters the reached p_C and thus T_C with varying compression times even if all other parameters are held constant. Further, a potential radical build-up during compression could be of interest, as it could affect p_C (T_C) and the measured IDT. To define the compression time, two definitions, called τ_C [15] for the complete compression, and τ_{50} [2] for the last 50% of compression, can be found in the literature. In the case of τ_C, the authors suggest that the measured IDTs should be equal to or greater than τ_C, assuming that a relevant radical build up should be avoided if the IDT is larger than τ_C. However, to the best of the authors knowledge, no experimental evaluation of this definition exists in the literature.

In general, facility effects depend on several RCM operation parameters as the compression speed, the gas mixture composition, the temperature difference between gas and walls, and the geometry of the dead volumes. Even small change in operating conditions [16] can lead to significant differences in measured IDTs in different RCMs at seemingly the same end of compression conditions.

To understand these differences, it is important to point out that the measured IDT is the result of the entire pressure and temperature history of an RCM experiment and it does not depend solely on the EOC condition that are commonly reported. While this does not affect the validity of individual experiments or their corresponding simulations, it might lead to a misinterpretation that results from different RCMs are not comparable [17].

To address this issue and gain further understanding, a project to investigate autoignition of isooctane in 13 different RCMs was initiated within the framework of the 1st RCM workshop. *Iso*-octane is a fuel with negative temperature coefficient (NTC) ignition behaviour [13] and was initially chosen to investigate how the 1st stage of ignition is reflected in different RCMs. It was found that "scatter" in IDTs increased in the NTC region. Potential explanations were found to be differences in heat and mass flow into the crevice and induced reactivity in the compression phase [2]. The size and complexity of the fuel, the influence of the compression phase as well as the crevice and RCM design revealed that a more rigorous specification of the initial and boundary conditions was needed [2] and the overall complexity of the fuel investigated should be reduced in a future study.

Hence, to reduce the complexity in experimental and modelling efforts ethanol was chosen as a candidate for a combined effort to investigate and further understand differences in RCMs. Ethanol, C_2H_5OH, is a smaller molecule and only shows Arrhenius-type ignition behaviour in RCM experiments, i.e., it does not have any NTC region. This reduces the complexity of the problem and allows the separation of different factors affecting ignition behaviour.

Motivated by this initiative, a companion study to this one was carried out, in which ethanol was extensively studied in one RCM [16]. This companion study focused on two major aspects: varying experimental conditions (p_C, T_C, ϕ, dilution) over a wide range and varying the operational conditions of the RCM used. In this accompanying study it was found that a single kinetic model could replicate all of the experimental results, even those under vastly different operational conditions, within the machine's given uncertainty.

In the present study ethanol is investigated at a compressed pressure of 20 and 40 bar at stoichiometric conditions and at two different dilutions using five independent RCMs, including the facilities at Argonne National Laboratory (ANL), King Abdullah University of Science and Technology (KAUST), the University of Galway (UoG), RWTH Aachen University (HGD), and Lille University (Lille). Due to limitations in the maximum operating pressure, the experimental investigation in the RCM at Lille are limited to a compressed pressure of 20 bar. By comparing the results of all facilities, a better understanding of why and how experimental IDT data obtained in independent RCMs differ is obtained. It is important to note that RCMs are not standardized equipment, unlike the Cooperative Fuel Research (CFR) engine used for octane measurements (RON: ASTM D2699–18a [18], MON: ASTM D2700–18a [18]), and thus they have different configurations, different diagnostics (transducers and data acquisition systems), and different operating protocols or user behavior at each facility. A further goal of this study is to show that all experimental results from various facilities, albeit being different in a direct comparison, can be predicted using a single kinetic mechanism as the fuel chemistry is independent of the facility operation.

2. Methods

The basic working principle of the RCMs used in this joint-venture study is generally the same. In every facility a premixed fuel-oxidizer-mixture is rapidly compressed by a piston. Detailed mechanical descriptions of the RCMs used can be found in corresponding publications of each group (ANL: [19,20], KAUST: [21], UoG: [22], Lille [23]:, HGD: [24]. In the following section (Section 2.1) we focus on highlighting differences between the facilities. A consistent error propagation based on the work of Weber et al. [25] was carried out for all groups (Section 2.2). Furthermore, all contributed experimental data were re-evaluated with one common systematic approach starting from the raw data for every experiment. This ensures consistency in the thermodynamic properties used and in the data evaluation process. To be able to quantitatively compare different kinetic models with different experimental data sets, a performance metric has been developed which will be presented in Section 2.4.

2.1. Experimental facilities

A short summary of the distinguishing details of the RCMs used in this study is found in Table 1. In principle, IDTs are usually investigated in an RCM as a function of ϕ, dilution, p_C and/or T_C. Often, and also in the case of this study, data sets are measured by varying only one of the variables while the rest are kept constant. Usually, T_C is varied within

Table 1
Overview of RCMs used in this study.

Facility	T_C variation	Trajectory Control	N° of Pistons	τ_c / ms		τ_{50} / ms	
				min	max	min	max
ANL	T_i	Hydraulic, linear	2	12	22	1.2	2.4
KAUST	T_i	Hydraulic, linear	2	13	16	1.3	2.6
UoG	T_i	Hydraulic, linear	2	14	16	1.6	2.2
HGD	CR	Hydraulic, linear	1	15	23	2.4	4.8
Lille	γ	90° cam	1	33	38	5.0	5.4

one data set and multiple data sets are measured to obtain the influence of other variables such as p_C or ϕ. While ϕ and dilution are directly set by the chosen mixture composition and p_C is directly measured, T_C is a function of multiple variables, as shown in Eq. (1) given for an adiabatic compression [4]:

$$\int_{T_i}^{T_c} \frac{\gamma}{\gamma - 1} \cdot \frac{dT}{T} = ln(CR) \tag{1}$$

Eq. (1) shows that the initial temperature T_i, the isentropic exponent of the mixture γ and the compression ratio CR, i.e. the ratio between the top and bottom centre volumes, can be varied to achieve different values of T_C. Of these three variables, each is used by at least one of the contributing facilities, as summarized under "T_C variation" in Table 1. The different approaches inevitably lead to different facility effects. Varying only the initial temperature allows the heat loss parameters to be maintained, i.e., the heat transfer coefficient and the driving temperature difference between the core gas and the wall are nearly constant with the drawback of having longer heat-up times between experiments with different T_C. Changing the compression ratio permits a fast variation of experimental conditions but changes the reactor volume to surface area ratio so that heat loss effects become stronger at higher compression ratios. Varying γ requires the preparation of separate mixtures for each condition and the gas composition affects the heat transfer coefficients but this method avoids the need to vary initial temperatures.

Another aspect differentiating the machines is how the compression is achieved. Considering the energy balance of a closed system, the achievable compression in the core gas is reduced by the time-integrated heat flux into the reactor walls and the compression of dead-volumes compared to an ideal compression [3]. Consequently, the conditions in the RCM are also influenced by the compression time and the dead-volume to core gas volume ratio. The compression time can be characterized by τ_{50} or τ_C, whereby τ_{50} describes the time to achieve the last 50% pressure increase before the EOC while τ_C describes the entire compression time. Depending on other variables (i.e. driving pressure, T_{ini}, compression ratio, and the masses of moving parts) these times can vary within a machine as summarized by min/max values in Table 1. Generally, the twin piston systems (ANL, KAUST, UoG) show the shortest compression times. Compression times of the single piston machines (HGD, Lille) are higher, but have the benefit of a more reproducible compression stroke as variation in the piston synchronisation cannot influence the volume history.

Fixing the EOC is reached in two ways. The facilities at ANL, KAUST, UoG, HGD use the pneumatic force on the compression piston, which is greater than the force on the reactor piston. In the RCM at Lille, the compression piston is mechanically locked in position by a 90° cam system. A hydraulic lock is used in the ANL machine to resist extreme pressure forces.

The rate at which the EOC is reached directly influences the achievable p_C and T_C for a given mixture composition. This means that in addition to the direct influence of the heat loss on the IDT determined by the temperature-dependent kinetics, the referenced variables (p_C, T_C) specified for the respective IDT are also influenced by facility effects. This means that a direct comparison of experimental results from different facilities at the same reference conditions of p_C and T_C is not valid since the results stem from different pressure and temperature histories. However, as will be shown in the course of this study, when accounting for all the different facility effects properly, results agree to each other within their uncertainty limits.

2.2. Errors and uncertainties in experiments

Errors associated with RCM measurements were discussed by Sung and Curran [3] and Goldsborough et al. [2] and a detailed error propagation for T_C was conducted by Weber et al. [25]. Based on the python script provided by Weber et al. the error propagation on the determination of the core gas temperature was calculated in this study.

The use of calibrated sensor uncertainties requires that the sensor directly measures the desired physical quantity. If this is not the case and an indirect measurement is used, an additional error contribution must be considered. In RCM experiments such an indirect measurement is the measurement of the initial temperature T_i. The desired T_i is the gas phase temperature before compression and it directly influences the uncertainty of the compressed gas temperature which is the most critical parameter in the ignition process. However, the initial temperature is usually measured as a bulk temperature of the reactor by multiple sensors on the outside of the reactor or in pocket holes. Temperature differences between the gas phase and the bulk temperature can be caused by the filling process or by local temperature differences in the reactor especially towards unheated parts of the machine. A general applicable complication in heated RCMs is that the piston is generally unheated, and as shown by Wadkar and Toulson [26] can lead to significant differences in the bulk temperature and thus can increase the uncertainty in the initial temperature measurement.

Another aspect, which needs to be considered, is the dynamic pressure sensor used in the RCM. In case of this study, all facilities have used different types of piezoelectric pressure sensor (see supplemental material). Without any special request, these sensors are calibrated for engine specific conditions, e.g., 23 °C, 250 °C and 350 °C at operating pressures up to 100, 200, and 300 bar. For each condition a sensitivity and an uncertainty are provided by the manufacturer. However, neither the temperature nor the pressure range matches the conditions typically encountered in RCMs (typically T_i = 50 to 150 °C, p_C = 10 to 50 bar). Using a sensor outside of its calibrated conditions will add higher uncertainties to the measurements.

Furthermore, the data acquisition system, including the A/D card and other hardware, affect the accuracy and resolution of the data. The bit resolution of the card, sampling frequency, and any internal (e.g., integral to the card) or external filtering or smoothing can alter the measurements. The influence of these is hard to quantify and almost never reported.

To evaluate the potential effects of the uncertainties in the initial temperature in combination with the uncertainties on the dynamic pressure measurements, an exemplary error propagation analysis for the RCM at HGD was performed. For this exercise, gas phase temperatures were directly measured by several thermocouples to compare with the temperature measurement usually performed on the reactor walls. Furthermore, a pressure sensor calibration at the particular conditions of interest (75 °C, 50 bar) was performed by the manufacturer and compared to the standard calibration. The comparison between the gas phase and reactor bulk temperature measurement showed differences up to ± 1 K in the initial temperature. Furthermore, due to the off-condition calibration of the dynamic pressure sensor an additional uncertainty of 1% in the pressure measurement is observed. Using the gas phase temperature calibration and the specific calibration for the dynamic pressure sensor, an overall uncertainty of ± 0.4% in the compressed temperature for a 20 bar in-air dataset (e.g., 850 ± 3.3 K) was

computed using the error propagation method of Weber et al. [25]

Without specific pressure sensor calibrations as well as a gas-phase temperature calibration we recommend to assume the uncertainty of the measurements to be a factor of two higher compared to the nominal sensor uncertainty values. This would result in an overall uncertainty of the compressed gas temperature of approximately ± 1.0%. This order of magnitude in uncertainty agrees well with the results of Weber et al. [25] (< 0.7%) and the conservative estimations of Fridlyand et al. (± 0.5% to ± 1.5%) [19] and Goldsborough et al. (± 1.5%) [27].

Using nominal sensor uncertainties in uncertainty analyses for the other RCMs of this study results in values (Tab. 2) ranging between 0.4 and 0.66%. Hence, for a conservative estimation of the uncertainty that considers the potential issues in gas phase and pressure sensor calibration, an average uncertainty of ± 1% in T_C is assumed in the following figures and indicated by a grey shaded area for all groups. This uncertainty in the compressed gas temperature might be transferred into an uncertainty in ignition delay time using the temperature dependency observed in the experiments. This results in an uncertainty in the IDTs of 25% to 30% depending on the slope of the corresponding data set. Overall, this conservative uncertainty leads to slightly higher values than the often-estimated uncertainties of approximately 20% [28–32].

2.3. Simulation approach

RCM experiments are conventionally simulated using the effective volume approach, as described in [1,2,7,13,24,33]. Briefly, in this approach an accompanying non-reactive experiment at each T_C is conducted. In the non-reactive mixture, oxygen is replaced by nitrogen rendering the experiment typically inert at RCM compressed temperatures where pyrolysis can usually be neglected. This non-reactive experiment encounters similar facility effects as the reactive experiment, and hence can be used as a "finger-print" by converting the pressure trace of the non-reactive experiment to an effective volume. This effective volume is then prescribed in the kinetic simulation.

However, a variation between the reactive and non-reactive experiments can occur depending on the working principles of the RCMs, which can lead to differences in the simulated and measured conditions. This can lead to a bias in the evaluation when comparing IDTs at slightly different temperatures and pressures in experiment and simulation. Therefore, to avoid this effect, another approach has been adapted from the studies of Dames et al. [34] and Weber et al. [33] wherein reactive and non-reactive pressure traces are combined. In this approach the pressure profile of the compression phase of a reactive experiment is combined with the heat loss phase of its corresponding non-reactive counterpart. This then results in individual non-reactive pressure traces which are used to create the effective volume files used in later simulations. The EOC conditions achieved in the reactive experiments are matched in the simulations and each experimental IDT can be directly compared to the corresponding simulated IDT without the need of any further fits or subjective interpretations. This approach can be used as long as chemical reactions during the compression phase do not significantly influence the pressure history which is typically the case for longer IDTs.

2.4. Performance metrics

To be able to compare different models with each other and the agreement between the data sets of different groups with a common model, an unbiased numeric performance metric had to be defined. The simplest stochastic approach used is the mean percentage error (*MPE* or $\overline{\delta IDT}$) and the mean absolute percentage error (*MAPE* or $|\overline{\delta IDT}|$) as defined below:

$$MPE \vee \overline{\delta IDT} = \frac{100\%}{n} \cdot \sum_{t=1}^{n} \frac{IDT(exp)_t - IDT(sim)_t}{IDT(exp)_t}$$

$$MAPE \vee |\overline{\delta IDT}| = \frac{100\%}{n} \cdot \sum_{t=1}^{n} \left| \frac{IDT(exp)_t - IDT(sim)_t}{IDT(exp)_t} \right|$$

With $IDT(exp)$ being the actual experimental IDT and $IDT(sim)$ being the simulated IDT at the same EOC conditions over n varying conditions.

While *MAPE* can give a good overview of the general predication accuracy, it leads to an asymmetric bias meaning that it will put a slightly heavier penalty on negative errors [35]. Therefore, using *MAPE* as a direct comparison between models or dataset could lead to a distortion of the actual performance.

A simple approach to correct this and obtain a symmetric relative error (*sRE* or $sym.\overline{\delta IDT}$) is to calculate an error as described in [36]:

$$sRE \vee sym.\overline{\delta IDT} = \frac{100\%}{n} \cdot \sum_{t=1}^{n} ln\left(\frac{IDT(exp)_t}{IDT(sim)_t}\right)$$

Overall the value will be close to value of *MAPE* and hence allow for the same intuitive interpretation but without the directed bias. Similar to *MPE/MAPE* a symmetric absolute error ($|sRE|$ or $|sym.\overline{\delta IDT}|$) can be achieved when summing over the absolute values of the ln-function.

2.5. Kinetic models

There are several chemical kinetic combustion mechanisms that include ethanol as well as mechanisms that have been developed explicitly for ethanol. For this study a total of four previously published models [Mittal et al. [14], NUIGMech1.1 [37,38], CRECK_2003_TPRF_HT_LT_ALC [39–41], Zyada et al. [42]) and the model from the companion study (HGD V2) [16] have been tested against the experimental data of this study.

The mechanism of Mittal et al. and Zyada et al. are both ethanol specific models developed using experimental IDTs from their corresponding facilities and other experimental devices (i.e. ST, JSR). The other two mechanism are general or hierarchical models which have been validated against a variety of different IDT results, both from different RCMs and shock tubes (ST) as well as other validation targets (i.e. speciation from JSR), including fuels other than ethanol. The model from the companion paper is based on NUIGMech1.1 but is slightly modified to achieve a best fit to the data set from that study.

For the selected models, the thermodynamic data were not identical. This might stem from uncertainties in the applied method for deducing the thermodynamic data of the fuel (experiment, quantum mechanical calculation, or group additivity method). Remarkably, these differences in the heat capacity can lead to differences of T_C of up to 5 K.

To ensure consistency when comparing simulations against experiments, each experimental T_C and the effective volume profiles have been re-evaluated using the thermodynamic data from the corresponding mechanism. Hence, in all shown plots, the IDTs of experiments and simulations are always based on the used mechanism. This explains why the same experiments are shown in the different plots at slightly different reference temperatures.

In addition to the evaluation of kinetic mechanisms from literature an optimized model has been developed. The aim was to evaluate whether one mechanism would be able to predict all data within the experimental uncertainty. Unlike the model developed in the first part of this work [16] this time the optimization was not performed manually but a linear optimizer was used [43] in order to avoid any user bias. It is important to note that the goal of this model optimization is not to find the best kinetic mechanism for ethanol oxidation. In contrast, the goal of this study is to evaluate to what degree the results of the different RCM experiments agree with each other by comparing them to the optimized model. The linear optimizer was set to initially conduct a sensitivity analysis for all reactions of the ethanol sub mechanism included in the NUIGMech1.1 to identify the reactions that influence the system most. NUIGMech1.1 was chosen as starting point since it showed the lowest mean deviation as will be discussed subsequently.

Fig. 1 shows IDT sensitivity coefficients of the ten most sensitive fuel specific reactions for the target conditions in the validation pool. $P\dot{C}_2H_4OH$ denotes the primary ethanol radical and $S\dot{C}_2H_4OH$ the secondary radical accordingly. $C_2H_5\dot{O}$ describes the ethanol radical after H-atom abstraction on the alcohol site. The sensitivity coefficient S is defined as: $S = \ln(IDT+/IDT-)/\ln(2/0.5)$ [44]. Most of the reactions are H-atom abstraction reactions from ethanol by $\dot{O}H$, $H\dot{O}_2$, $CH_3\dot{O}_2$ and O_2. Furthermore, H-atom abstraction from acetaldehyde (CH_3CHO) and β-scission of the ethanol radical formed after H-atom abstraction on the alcohol site ($C_2H_5\dot{O}$) are sensitive. For the entire regime of investigated conditions within this study sensitivities remain about the same. In NUIGMech1.1, H-atom abstractions by $H\dot{O}_2$ radicals are estimated by analogy with the Zhou et al. [45] study on *n*-butanol. H-atom abstractions by $CH_3\dot{O}_2$ radicals are estimated in analogy to the rate parameters for abstraction by $H\dot{O}_2$. Initiation reactions, i.e. ethanol + O_2, are taken from the work of Sivaramakrishnan et al. [46]. H-atom abstraction by $\dot{O}H$ has been deduced from the same work but slightly modified as described in the work of Metcalfe et al. [47]. For the quantum mechanical calculations presented in [40] uncertainties in the rate coefficients are estimated to be a factor of 2–3. Consequently, all uncertainties for the rates derived from these calculations are expected to be at least a factor of two which is used as maximum limit during the model optimization procedure. Further details of ethanol oxidation chemistry are discussed in previous studies [14,48]

To create a fair and unbiased validation dataset that is not influenced by the number of provided experiments of the different participating groups, two representative experiments, one experiment with an IDT around 10 ms and another around 100 ms, per dataset and group were added. The optimizer was allowed to vary the Arrhenius parameters *A, n* and E_a of the ten most sensitive fuel specific reactions with the restriction that the resulting reaction rate does not deviate more than a given factor. This factor was increased in an iterative process from 1.3 to 2.0. The model improved from 1.3 up to 1.6, but there was no further noticeable improvement for higher values. To reduce the amount of change applied to the model the optimized model with a maximum alteration factor of 1.6 was used. The optimization target was set to reduce the overall absolute *sRE* of all groups.

Of the ten modified reactions, nine were modified by *A*-factor variation in the range of 1.46–1.59. Only the most reactivity decreasing reaction, the H-atom abstraction by $\dot{O}H$ radical on the secondary site, was altered in *A, n* and E_a. A comparison of the original and changed rate coefficients can be found as Supplementary material.

3. Results

3.1. Experimental results of all groups

In the course of this study ethanol was investigated at two compression pressures (p_C = 20 and 40 bar) and two dilutions (oxygen/diluent ratio: 79/21 denoted as 'in-air' and 88/12 denoted as 'diluted').

Fig. 2 exemplarily shows the measured IDTs of all facilities at 20 bar in air. For all data sets an Arrhenius type ignition behaviour can be observed as expected and an Arrhenius correlation is fitted for the individual data sets. This allows the evaluation of data scatter and an easier evaluation of trends in the later discussion. Similar to the symmetric error *sRE* between experiments and simulations a symmetric error sRE_{Arr} between experiments and their corresponding Arrhenius fit can be calculated. The mean deviation between experiments and their corresponding Arrhenius fit is $|sRE_{Arr}| < 6.5\%$ for the 20 bar, in-air conditions, and $|sRE_{Arr}| < 5.7\%$ for the 20 bar, diluted conditions. The level of the scatter of data is similar between the different facilities and might stem from slight variations in initial conditions, compressed conditions, statistic error, facility operation or weak inhomogeneous ignition effects which are difficult to predict or quantify.

For a more comprehensive comparison of the results from different facilities the exponential fits of the data sets are displayed against each other in the following figures. Figures of the raw data of all other data sets against the exponential fit are available as Supplementary material.

Fig. 3 shows a comparison of all experimental fits of all facilities for the two 20 bar data sets. The simulations are carried out using the optimized model described in detail later. Throughout the investigated conditions the results from the different machines show similar behaviour and ignition delay times are in a comparable order of magnitude for the same conditions. However, there are obvious differences in the ignition behaviour. First looking at the 20 bar in-air data (Fig. 3), the slopes of the exponential fits are very similar, but the results from KAUST closely followed by HGD show the longest IDTs (lowest reactivity) while the results from Lille show the shortest IDT. The differences in IDT between these two extremes amount up to 65% in IDT. At the same pressure level but higher dilution (Fig. 3) the results from UoG tend to have the longest IDTs, while the results from HGD are now the second fastest. Only the IDTs from Lille remain at its previous position. Further, a difference in the slope of the fit from the results from ANL is noticeable.

Overall, the differences within a dataset as well as the changing

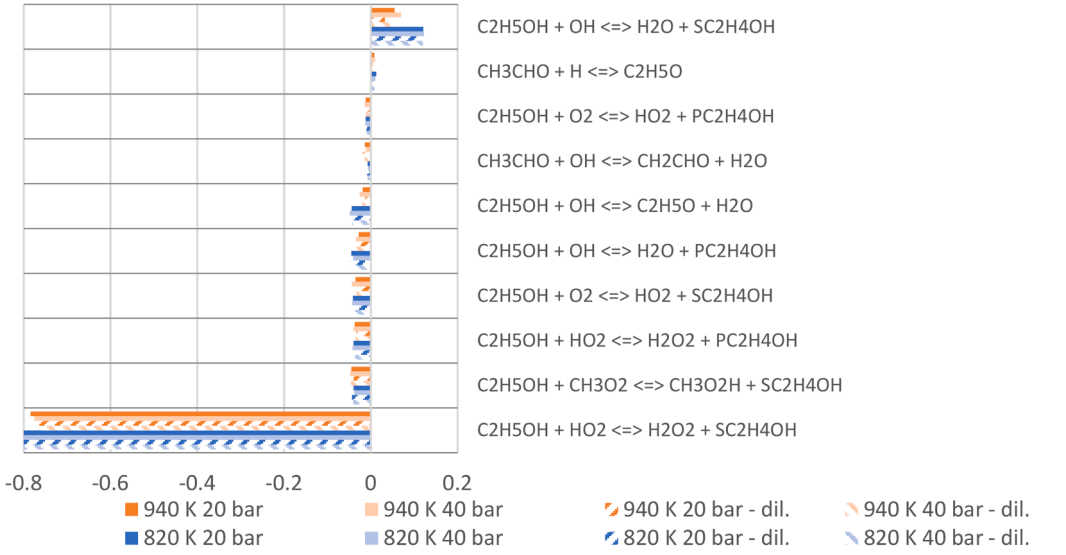

Fig. 1. Sensitivity analysis of the reaction rate K. $S = \ln(IDT+/IDT-)/\ln(2/0.5)$. A negative value denotes a reactivity increasing reaction, a positive value a reactivity decreasing reaction.

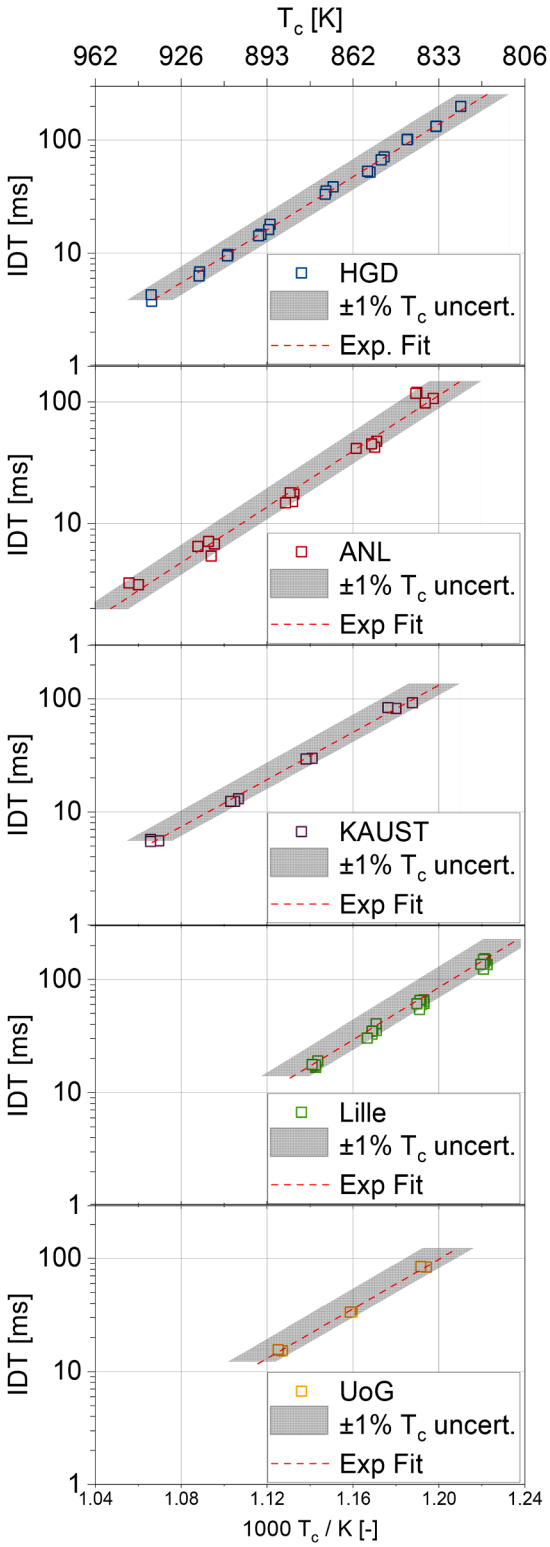

Fig. 2. Individual experimental results for 20 bar, in-air data sets of all five contributing groups. For each data set an Arrhenius fit was found and is shown as dotted red line. The grey shaded area describes the expected uncertainty in T_C in respect to the Arrhenius fit.

"ranking" between the data sets can be explained by a) the different facility effects and b) uncertainties and errors of each facility. Both impacts are not a constant offset for each machine but depend on how the machine is operated and which parameters are varied to achieve the desired conditions.

While the details for the uncertainties are discussed in Section 2.2 the differences in the pressure traces and hence the facility effects will be discussed in the following. The traces differ mainly in two aspects: the compression phase and the heat loss phase.

As indicated by τ_{50} (Table 1) the experiment conducted in Lille's facility shows the slowest compression phase followed by HGD, UoG, and KAUST (cf. Fig. 4 left). A slow compression phase leads to a longer time period at increased pressures and temperatures before EOC is reached. This reactivity-influencing period can also be considered as effective pressure or temperature. With a higher effective pressure and temperature, the resulting IDT will be shorter. Furthermore, the pressure trace from Lille also shows the overall weakest pressure loss over time, which has its origin in the heat loss of the hot compressed gas to the reactor walls. This leads to higher temperatures after EOC compared to the other facilities. Combined, these two effects ultimately lead to shorter IDTs for the Lille facility at apparently the same EOC conditions.

The results from KAUST and HGD show the overall longest ignition delay times for the 20 bar in-air data whereby at the highest investigated temperatures the IDTs from KAUST are even longer than the ones form HGD. This trend seems to correlate to the pressure traces of HGD and KAUST. The facility at KAUST exhibits a faster compression compared to HGD, hence a lower effective pressure and temperature. After the end of compression, the pressure profile from KAUST shows a slightly higher pressure drop rate which might be caused by weak piston rebound or other effects such as delayed gas flow into dead volumes. Dedicated investigations would be required to identify the root cause for the higher pressure drop rate. The faster compression and the higher pressure drop after EOC together lead to longer IDTs. For long measurement times the effect of the compression phase and potential piston rebound do not affect IDT significantly and the obtained IDTs from KAUST and HGD are similar.

IDTs from UoG and ANL are in between those of the other facilities in case of the 20 bar in-air experiments. Here the differences cannot be explained only on the basis of the pressure profiles. The last part of the compression phase from both machines is very similar to the behaviour of the facility at KAUST. From this, similar amounts of reactivity prior to EOC can be expected in all three dual-piston machines. Consequently, at least for short ignition delays the observable IDTs should be similar. Immediately after the EOC the pressure drops fastest in the UoG machine, but it decreases less than the other two for longer measuring times. The initial faster pressure drop might be an indication for piston rebound or gas flow into dead volumes as mentioned before. Again, further investigations would be required to specify the reasons for the observed pressure histories which is outside the scope of this study. The lower pressure drop in the later phase might stem from the higher volume to surface ratio in the UoG machine. Considering the energy balance of a closed system and assuming a constant heat flux density a lower surface area or a higher gas volume leads to a lower heat loss induced pressure decrease in the system. The higher initial but lower later pressure decrease leads to slightly longer IDTs for short measuring times but shorter IDTs for longer measuring times. This can be observed in the slightly higher global activation energy of the measured IDTs at UoG compared to ANL or KAUST (Fig. 3a). However, this qualitative analysis of the pressure traces only describes trends that can be expected from the differences in facility behaviour. Remaining differences in the comparison between the machines are likely due to measurement uncertainties.

In case of the diluted conditions at 20 bar, the pressure traces shown in the right plot in Fig. 4 show the slowest compression phase and the lowest pressure drop due to heat loss for the Lille facility, which explains the resulting fastest IDTs. The pressure traces from HGD have changed compared to the in-air condition. In this case the compression phase is slightly slower, becoming more similar to the compression of the Lille RCM and likewise the heat loss becomes less and more alike to that of Lille. This explains why HGD IDTs at diluted conditions are now the second fastest, close to the results of Lille in both reactivity and slope.

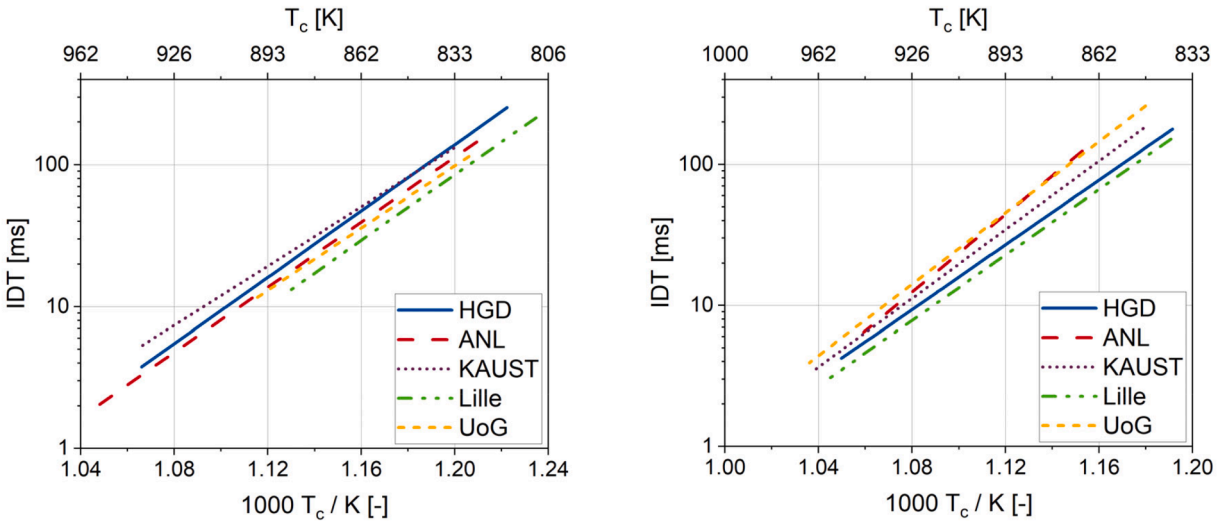

Fig. 3. Overview of exponential experimental fits for ethanol IDTs at 20 bar, in-air (left) and 20 bar, diluted (right) conditions.

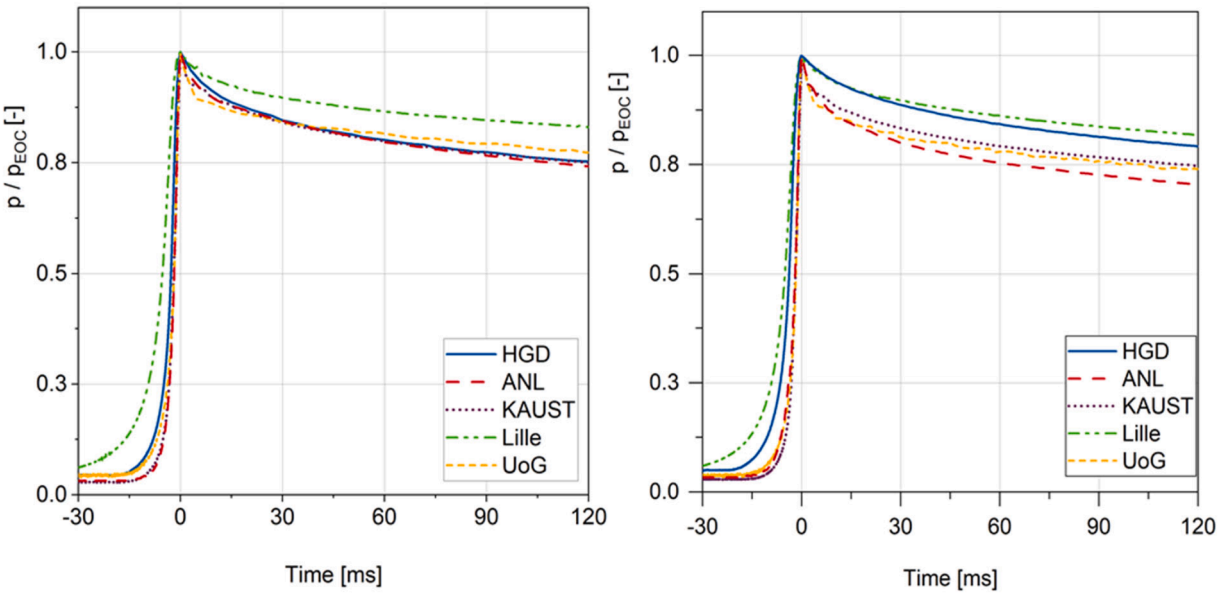

Fig. 4. Normalized non-reactive pressure traces of the different facilities. Left: 20 bar, in-air conditions at ca. 840 K Right: 20 bar, diluted conditions at ca. 850 K.

The reason for this change within the HGD facility is that different compression ratios were used for the diluted and in-air conditions. For the diluted conditions, a smaller compression ratio was needed due to lower fuel concentration and therefore lower heat capacity of the mixture compared to the in-air conditions to reach the same EOC conditions. With a lower compression ratio, a slower compression is induced and with a higher volume to surface ratio the impact of the heat loss is reduced.

In contrast to the in-air conditions the pressure remains the highest in the KAUST facility compared to the results from UoG and ANL after the end of compression. This results in higher temperatures and consequently the measured IDTs (Figs. 2 and 3) are consistently shorter than the ones from UoG or ANL for the diluted mixture at 20 bar EOC. Similar trends as discussed above can be seen also for 40 bar EOC pressure. This analysis is presented in the Supplementary material.

In summary, the described differences in the IDT results should all stem from the differences in the facility operation. In case of significant differences in the pressure traces at seemingly the same EOC conditions, as seen for the 20 bar diluted experiments, the observed differences in compression and heat loss align with the expectations based on the observed reactivity and the simulation results. However, when only minor differences between the pressure traces can be observed, uncertainties and errors of the different facilities impede a detailed interpretation and consequently the simulation results predict a different alignment between the facilities.

3.2. Simulation results

All 18 data sets of this study have been calculated using the aforementioned five models. An overview of all plots can be found in the supplemental material. An exemplary detailed discussion of one 20 bar in-air data set is included here to illustrate the analysis.

Fig. 5 shows experimental and simulated IDTs and their Arrhenius fits for the corresponding data set provided by ANL. The simulations are performed using NUIGMech1.1 in this case. As discussed before, the experimental data have some scatter but these are within the expected uncertainty range around the Arrhenius fit. The simulation results using the effective volume method [3,5] agree to the experiments within this

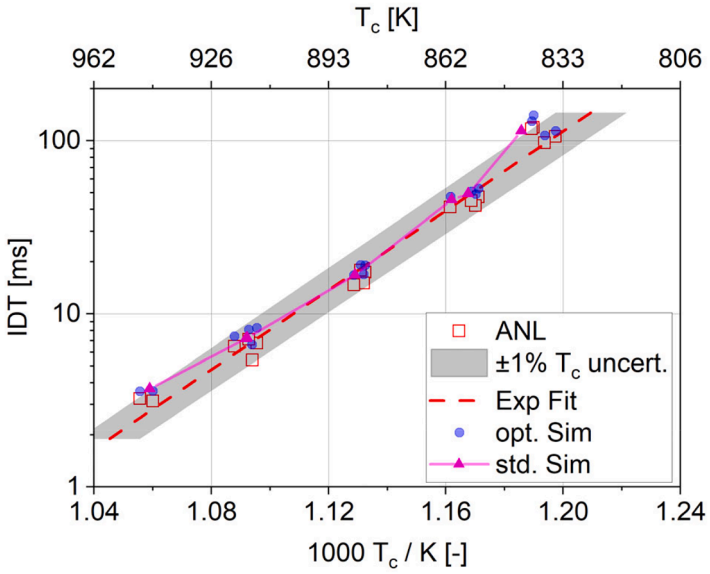

Fig. 5. Comparison of conventional and optimized simulation approach. Square symbols: experimental data from ANL at 20 bar in-air. Dashed line: experimental fit. Solid line with full triangles: conventional simulation results. Blue circles: optimized simulation approach. Grey shades: Tc uncertainty in respect to experimental fit.

range. It is important to note the differences in using the conventional effective volume profiles and the optimized effective volume profile as described before. Typically, one non-reactive pressure profile is used for deducing one characteristic volume profile for one condition. Due to slight differences between reactive and non-reactive experiments the end-of-compression conditions do not match entirely. These differences can stem from uncertainties in the initial filling of the machines, from slight differences in the thermodynamic properties of the reactive and non-reactive mixture, or from differences in the volume history induced, for example, by piston mis-synchronisation. These individual variation in the experiments cannot be accounted for in the simulation using only one representative volume profile for each reactive experiment, but can be compensated by the optimized effective volume approach. Using the compression phase pressure profile of each individual reactive experiment ensures to include potential variation in the facility behaviour in each simulation. Consequently, the simulations using the optimized effective volume approach should reflect the individual experiments better. This becomes clear comparing the agreement of the conventional and optimized simulation to the experiments. For the conventional approach an overall mean abs. *sRE* of ~ 14% is achieved while comparing individual experiments to the exponential fit of the simulation. The simulations using the optimized approach better follow the variation in the experimental conditions as well as measured IDTs and consequently a lower mean abs. *sRE* of 11.8% is achieved by directly comparing each experiment to its matching simulation. While the difference in the average error is not very high, the discrepancy between experiment and conventional simulation can become larger for individual conditions. This becomes apparent looking at the experiments at 840 K where the conventional simulation deviates significantly from the two experiments at the lowest temperatures while the optimized approach can reflect these experiments well. In other words, this observation demonstrates that the variation of the IDT at the same target conditions is not due to a random scatter but rather induced to variation in the facility behaviour which can be accounted for in simulation.

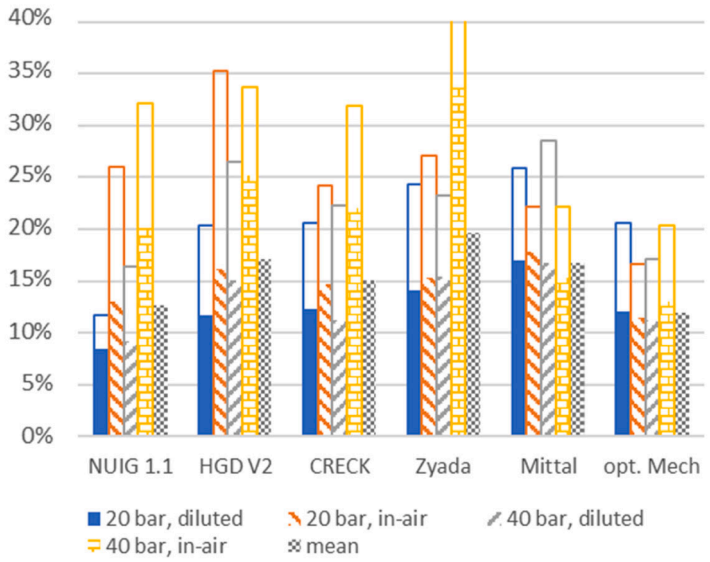

Fig. 6. Mean absolute sRE averaged over all data sets per condition/group for the 6 different models used in this study (full bars). Max. deviation shows the highest mean absolute sRE for a single data set (transparent bars).

Due to the better performance of the simulations using the optimized effective volume profiles, this method has been used for all subsequent simulations. Fig. 6 displays an overview of the mean absolute *sREs* of each mechanism averaged over all data sets of each condition, resulting in a variation of 8–34% for the different mechanisms which is close to the expected uncertainty.

In these averaged results (full bars) no obvious outlier is identified in experiment. However, looking at the individual data sets, i.e., a temperature sweep at constant pressure and mixture composition, significantly higher maximum deviations can be observed, as highlighted by the transparent bars in Fig. 6. This is especially true for the mechanism of Zyada et al. where the maximum deviation amounts to 55%. This relatively high deviation might be due to the fact that this mechanism has been optimized against experiments in the RCM regime with diluted conditions only. Thus, conditions with high fuel concentrations, such as fuel-air mixtures at 40 bar EOC, are outside the validated regime for this mechanism. However, other mechanisms also show maximum *sREs* of individual data sets that are outside the expected experimental uncertainty. These differences between simulation and experimental results do not allow one to conclude on the quality of individual RCM experiments as none of the mechanisms can be considered fully valid. Nonetheless, the common ground in all experiments is the oxidation chemistry of ethanol that does not differ between the different machines. Thus, it should be possible to find one kinetic mechanism that describes all data sets within the experimental uncertainty given that our understanding of the facility behaviour and simulation techniques for the RCMs is correct.

This has been attempted by developing the optimized kinetic model. As discussed before, all changes in the rate coefficients during the model optimization process are well within the uncertainty of each reaction. The simulation results using this mechanism show a slight improvement of the mean absolute sRE of 11.9% compared to 12.5% of the original NUIGMech1.1 as summarized in Fig. 6 (full bars). While an improvement of 0.6% points of the abs. sRE seems hardly remarkable, the improvement of the model is clearly visible by the reduction in maximum deviation of the data sets (transparent bars). NUIGMech1.1 showed a maximum deviation up to 32% for the 40 bar in air case, the optimized model can predict all data sets within ± 21%. The latter is well within the expected experimental uncertainty and close to the often-provided estimation for IDT measurement uncertainty of 20% in RCMs. When comparing the mean values of the highest deviating datasets, the optimized mechanism improves from 21.6% to 18.7%. Furthermore, the level of agreement also shows that the conventionally used simulation approach using effective volume profiles is suitable to describe the variation in facility behaviour of independent machines. However, it is important to note that this high level of agreement was achieved by considering all data sets from the five different facilities for model optimization. The optimized kinetic model represents the average of all RCMs and all results fall into $a \pm 21\%$ uncertainty band from this average. However, that also means that this range has a span of 42 percentage points. If the reference model is optimized to one extreme of this scatter band, data on the opposite extreme could show differences of up to 42%. If the optimization is done with a data set that is close to the average, the agreement of the other data would appear better. This can be seen in Fig. 6 where the optimized mechanism from the companion study (HGD V2) has been optimized to the results of only one machine and consequently maximum deviations of 35.3% against all experimental data of this study are observed.

The developed mechanism has also been tested against literature data from RCM [14], shock tube [49–51], and jet stirred reactor [52]. These comparisons together with simulation results of the unmodified NUIGMech1.1 are presented in the Supplemental Material. It can be seen that the optimized kinetic model changes the ignition prediction mainly in the RCM regime as discussed before. For shock tube and species measurements in JSR only minor differences to the original NUIGMech1.1 exist.

4. Conclusions

The major target of the present study was to understand the differences in IDT measurements when comparing the results from different rapid compression machines. Differences in the machine operation and design lead to different compression and heat loss characteristics. This changes the pressure and temperature history of the reacting gas in the RCM ultimately resulting in different IDTs at the same nominal end of compression conditions. According to the adiabatic core hypothesis the finite compression time and heat loss, which are also called facility effects, can be expressed as an effective volume change of an ideal 0-D reactor. Thus, by accounting for the effective volume change of the adiabatic core in chemical kinetic simulations, it should be possible to predict all experimental results by one kinetic model.

To confirm this hypothesis and to evaluate the level of agreement that can be achieved between different RCMs, ethanol IDTs at 20 and 40 bar for stochiometric mixtures in air like and an increased level of dilution were measured in five independent facilities. A systematic analysis of the facility behaviours and measurement uncertainties was carried out. Kinetic simulations with optimized effective volume profiles were performed with different mechanisms from literature. Furthermore, the unique data produced in the present study allowed optimizing a kinetic mechanism for RCM conditions. With this optimized mechanism, the highest level of agreement between simulations and experiments could be achieved.

The highlights of this work can be summarized as follows:

- Unique benchmark data on ethanol ignition delay time measurements obtained at 20–40 bar in five independent rapid compression machines
- In agreement to previous literature, ± 1% uncertainty in the compressed gas temperature can be expected. For ethanol ignition this uncertainty in temperature can be translated to an uncertainty in ignition delay time of 25–30% at a nominal temperature.
- Simulations using the effective volume approach and different kinetic mechanisms from literature showed reasonable trends for all data. However, single data sets, i.e. temperature sweeps at constant pressure and mixture conditions, showed deviation of up to 40% between simulations and experiments which is outside the expected measurement uncertainty.
- Based on the NUIGMech1.1, an automated model optimization was performed by considering representative data from the present study. Using the optimized kinetic model differences between simulation and experiment could be reduced to below 21% for each single data set. Even literature data that were not part of the optimization process are reflected well by the optimized mechanism.
- The high level of agreement between the optimized kinetic model and the experiments from different RCMs confirms that the effective volume simulation approach is capable of accounting for differences in facility effects of various machines. However, it is important to keep in mind that optimizing a kinetic model to just the results of a single facility can lead to an overall worse prediction of the entire data sets. Thus, highest level of confidence in a kinetic model can be only achieved if measurements at the same conditions from different independent machines are considered for model optimization. This does not only hold for RCMs but for several experimental techniques and thus places emphasis on repeating experimental conditions in various facilities to develop high quality kinetic mechanisms.

Novelty and significance statement

For the first time, ethanol ignition delay times from five independent RCMs with different designs and operating protocols were compared and analyzed in this work. Using the effective volume simulation approach, an optimized kinetic model is able to predict the ignition delay times from all facilities within ± 21%. The optimized mechanism

was even able to reproduce experimental results from literature which were not part of the optimization routine. This is the first study, that confirms that the validation of a kinetic model is independent of the corresponding facility if the boundary conditions of the experiments are accurately known and treated correctly during the simulation.

CRediT authorship contribution statement

R.D. Büttgen: Methodology, Visualization, Investigation, Validation, Writing – review & editing. **M. Preußker:** Investigation, Writing – review & editing. **D. Kang:** Investigation, Writing – review & editing. **S. Cheng:** Investigation, Writing – review & editing. **S.S. Goldsborough:** Project administration, Conceptualization, Funding acquisition, Resources, Supervision, Writing – review & editing. **G. Issayev:** Investigation, Writing – review & editing. **A. Farooq:** Project administration, Conceptualization, Funding acquisition, Resources, Supervision, Writing – review & editing. **H. Song:** Investigation, Writing – review & editing. **Y. Fenard:** Investigation, Writing – review & editing. **G. Vanhove:** Project administration, Conceptualization, Funding acquisition, Resources, Supervision, Writing – review & editing. **A. Abd El-Sabor Mohamed:** Investigation, Writing – review & editing. **H.J. Curran:** Project administration, Conceptualization, Funding acquisition, Resources, Supervision, Writing – review & editing. **K.A. Heufer:** Project administration, Conceptualization, Funding acquisition, Resources, Supervision, Writing – review & editing.

Declaration of competing interest

The authors declare that they have no known competing financial interests or personal relationships that could have appeared to influence the work reported in this paper.

Acknowledgments

The work of KAUST authors was sponsored by the Office of Sponsored Research at King Abdullah University of Science and Technology (KAUST). The work at ANL was performed under the auspices of the U.S. Department of Energy (DOE) under Contract DE-AC02–06CH11357 and was sponsored by the DOE Office of Energy Efficiency and Renewable Energy (EERE) Vehicle Technologies Office.

Supplementary materials

Supplementary material associated with this article can be found, in the online version, at doi:10.1016/j.combustflame.2024.113338.

References

[1] A. Kéromnès, Rapid compression machines, F. Battin-Leclerc, J.M. Simmie, E. Blurock (Eds.). Cleaner Combustion: Developing Detailed Chemical Kinetic Models, Springer, London, London, UK, 2013, pp. 163–181.
[2] S.S. Goldsborough, S. Hochgreb, G. Vanhove, M.S. Wooldridge, H.J. Curran, C. J. Sung, Advances in rapid compression machine studies of low- and intermediate-temperature autoignition phenomena, Prog. Energy Combust. Sci. 63 (2017) 1–78.
[3] C.J. Sung, H.J. Curran, Using rapid compression machines for chemical kinetics studies, Prog. Energy Combust. Sci. 44 (2014) 1–18.
[4] H. Hu, J. Keck, Autoignition of adiabatically compressed combustible gas mixtures, SAE Trans. (1987) 592–604.
[5] D. Lee, S. Hochgreb, Rapid compression machines: heat transfer and suppression of corner vortex, Combust. Flame 114 (1998) 531–545.
[6] G. Mittal. A rapid compression machine: design, characterization, and autoignition investigations, Ph.D. Thesis, Case Western Reserve University, 2006.
[7] R.D. Büttgen, T. Raffius, G. Grünefeld, H.J. Koß, A. Heufer, High-speed imaging of the ignition of ethanol at engine relevant conditions in a rapid compression machine, Proc. Combust. Inst. 37 (2019) 1471–1478.
[8] G. Mittal, M.P. Raju, C.J. Sung, Computational fluid dynamics modeling of hydrogen ignition in a rapid compression machine, Combust. Flame 155 (2008) 417–428.
[9] G. Mittal, M.P. Raju, C.J. Sung, CFD modeling of two-stage ignition in a rapid compression machine: assessment of zero-dimensional approach, Combust. Flame 157 (2010) 1316–1324.
[10] R. Minetti, M. Carlier, M. Ribaucour, E. Therssen, L. Sochet, Comparison of oxidation and autoignition of the two primary reference fuels by rapid compression, Symp. Int. Combust. 26 (1996) 747–753.
[11] J.F. Griffiths, P.A. Halford-Maw, C. Mohamed, Spontaneous ignition delays as a diagnostic of the propensity of alkanes to cause engine knock, Combust. Flame 111 (1997) 327–337.
[12] E.J. Silke, H.J. Curran, J.M. Simmie, The influence of fuel structure on combustion as demonstrated by the isomers of heptane: a rapid compression machine study, Proc. Combust. Inst. 30 (2005) 2639–2647.
[13] G. Mittal, C.J. Sung, A rapid compression compression machine for chemical kinetics studies at elevated pressures and temperatures, Combust. Sci. Technol. 179 (2007) 497–530.
[14] G. Mittal, S.M. Burke, V.A. Davies, B. Parajuli, W.K. Metcalfe, H.J. Curran, Autoignition of ethanol in a rapid compression machine, Combust. Flame 161 (2014) 1164–1171.
[15] K.P. Grogan, S. Scott Goldsborough, M. Ihme, Ignition regimes in rapid compression machines, Combust. Flame 162 (2015) 3071–3080.
[16] M. Preußker, R.D. Büttgen, M.R. Noé, A. Heufer, Finding a common ground for RCM experiments. Part A: on the influences of facility effects regarding the reliability of experimental validations, Combust. Flame 262 (2024) 113323.
[17] C. Wadkar, P. Chinnathambi, E. Toulson, Analysis of rapid compression machine facility effects on the auto-ignition of ethanol, Fuel 264 (2020) 116546.
[18] ASTM D2699-18a. Standard Test Method for Research Octane Number of Spark-Ignition Engine Fuel, ASTM International, West Conshohocken, 2018.
[19] A. Fridlyand, S.S. Goldsborough, M. Al Rashidi, S.M. Sarathy, M. Mehl, W.J. Pitz, Low temperature autoignition of 5-membered ring naphthenes: effects of substitution, Combust. Flame 200 (2019) 387–404.
[20] T. Rockstroh, A. Fridlyand, S. Ciatti, W. Cannella, S.S. Goldsborough, Autoignition behavior of a full boiling-range gasoline: observations in RCM and GCI engine environments, Combust. Flame 209 (2019) 239–255.
[21] G. Issayev, S. Mani Sarathy, A. Farooq, Autoignition of diethyl ether and a diethyl ether/ethanol blend, Fuel 279 (2020) 118553.
[22] W.S. Affleck, A. Thomas, An opposed piston rapid compression machine for preflame reaction studies, Proc. Inst. Mech. Eng. 183 (1968) 365–387.
[23] H. Song, R. Dauphin, G. Vanhove, A kinetic investigation on the synergistic low-temperature reactivity, antagonistic RON blending of high-octane fuels: diisobutylene and cyclopentane, Combust. Flame 220 (2020) 23–33.
[24] A. Ramalingam, K. Zhang, A. Dhongde, L. Virnich, H. Sankhla, H. Curran, A. Heufer, An RCM experimental and modeling study on CH4 and CH4/C2H6 oxidation at pressures up to 160bar, Fuel 206 (2017) 325–333.
[25] B.W. Weber, C.J. Sung, M.W. Renfro, On the uncertainty of temperature estimation in a rapid compression machine, Combust. Flame 162 (2015) 2518–2528.
[26] C. Wadkar, E. Toulson, CFD study of the effect of initial temperature inhomogeneities and buoyancy on the autoignition behavior of ethanol in an RCM, Energy Fuels 35 (2021) 17876–17889.
[27] S.S. Goldsborough, S. Cheng, D. Kang, C. Saggese, S.W. Wagnon, W.J. Pitz, Effects of isoalcohol blending with gasoline on autoignition behavior in a rapid compression machine: isopropanol and isobutanol, Proc. Combust. Inst. 38 (2021) 5655–5664.
[28] S. Jacobs, M. Döntgen, A.B.S. Alquaity, W.A. Kopp, L.C. Kröger, U. Burke, H. Pitsch, K. Leonhard, H.J. Curran, K.A. Heufer, Detailed kinetic modeling of dimethoxymethane. Part II: experimental and theoretical study of the kinetics and reaction mechanism, Combust. Flame 205 (2019) 522–533.
[29] S.M. Burke, U. Burke, R. Mc Donagh, O. Mathieu, I. Osorio, C. Keesee, A. Morones, E.L. Petersen, W. Wang, T.A. DeVerter, M.A. Oehlschlaeger, B. Rhodes, R. K. Hanson, D.F. Davidson, B.W. Weber, C.J. Sung, J. Santner, Y. Ju, F.M. Haas, F. L. Dryer, E.N. Volkov, E.J.K. Nilsson, A.A. Konnov, M. Alrefae, F. Khaled, A. Farooq, P. Dirrenberger, P.A. Glaude, F. Battin-Leclerc, H.J. Curran, An experimental and modeling study of propene oxidation. Part 2: ignition delay time and flame speed measurements, Combust. Flame 162 (2015) 296–314.
[30] J.G. Rittig, M. Ritzert, A.M. Schweidtmann, S. Winkler, J.M. Weber, P. Morsch, K. A. Heufer, M. Grohe, A. Mitsos, M. Dahmen, Graph machine learning for design of high-octane fuels, AlChE J. 69 (2022) e17971.
[31] U. Burke, J. Beeckmann, W.A. Kopp, Y. Uygun, H. Olivier, K. Leonhard, H. Pitsch, K.A. Heufer, A comprehensive experimental and kinetic modeling study of butanone, Combust. Flame 168 (2016) 296–309.
[32] S. Dong, K. Zhang, E.M. Ninnemann, A. Najjar, G. Kukkadapu, J. Baker, F. Arafin, Z. Wang, W.J. Pitz, S.S. Vasu, S.M. Sarathy, P.K. Senecal, H.J. Curran, A comprehensive experimental and kinetic modeling study of 1- and 2-pentene, Combust. Flame 223 (2021) 166–180.
[33] B.W. Weber, J.A. Bunnell, K. Kumar, C.J. Sung, Experiments and modeling of the autoignition of methyl pentanoate at low to intermediate temperatures and elevated pressures in a rapid compression machine, Fuel 212 (2018) 479–486.
[34] E.E. Dames, A.S. Rosen, B.W. Weber, C.W. Gao, C.J. Sung, W.H. Green, A detailed combined experimental and theoretical study on dimethyl ether/propane blended oxidation, Combust. Flame 168 (2016) 310–330.
[35] S. Makridakis, Accuracy measures: theoretical and practical concerns, Int. J. Forecast. 9 (1993) 527–529.
[36] C. Tofallis, A better measure of relative prediction accuracy for model selection and model estimation, J. Oper. Res. Soc. 66 (2015) 1352–1362.
[37] Y. Wu, S. Panigrahy, A.B. Sahu, C. Bariki, J. Beeckmann, J. Liang, A.A. E. Mohamed, S. Dong, C. Tang, H. Pitsch, Z. Huang, H.J. Curran, Understanding the antagonistic effect of methanol as a component in surrogate fuel models: a case study of methanol/n-heptane mixtures, Combust. Flame 226 (2021) 229–242.

[38] A. Ramalingam, S. Panigrahy, Y. Fenard, H. Curran, K.A. Heufer, A chemical kinetic perspective on the low-temperature oxidation of propane/propene mixtures through experiments and kinetic analyses, Combust. Flame 223 (2021) 361–375.
[39] E. Ranzi, A. Frassoldati, A. Stagni, M. Pelucchi, A. Cuoci, T. Faravelli, Reduced kinetic schemes of complex reaction systems: fossil and biomass-derived transportation fuels, Int. J. Chem. Kinet. 46 (2014) 512–542.
[40] E. Ranzi, C. Cavallotti, A. Cuoci, A. Frassoldati, M. Pelucchi, T. Faravelli, New reaction classes in the kinetic modeling of low temperature oxidation of n-alkanes, Combust. Flame 162 (2015) 1679–1691.
[41] G. Bagheri, E. Ranzi, M. Pelucchi, A. Parente, A. Frassoldati, T. Faravelli, Comprehensive kinetic study of combustion technologies for low environmental impact: MILD and OXY-fuel combustion of methane, Combust. Flame 212 (2020) 142–155.
[42] A. Zyada, O. Samimi-Abianeh, Ethanol kinetic model development and validation at wide ranges of mixture temperatures, pressures, and equivalence ratios, Energy Fuels 33 (2019) 7791–7804.
[43] T. Methling. Entwicklung des linearen transformationsmodells für die analyse und optimierung chemisch-kinetischer prozesse, Ph.D. Thesis, Universität Stuttgart, 2017.
[44] U. Burke, K.P. Somers, P. O'Toole, C.M. Zinner, N. Marquet, G. Bourque, E. L. Petersen, W.K. Metcalfe, Z. Serinyel, H.J. Curran, An ignition delay and kinetic modeling study of methane, dimethyl ether, and their mixtures at high pressures, Combust. Flame 162 (2015) 315–330.
[45] C.W. Zhou, J.M. Simmie, H.J. Curran, Rate constants for hydrogen abstraction by $H\dot{O}_2$ from n-butanol, Int. J. Chem. Kinet. 44 (2012) 155–164.
[46] R. Sivaramakrishnan, M.C. Su, J.V. Michael, S.J. Klippenstein, L.B. Harding, B. Ruscic, Rate constants for the thermal decomposition of ethanol and its bimolecular reactions with OH and D: reflected shock tube and theoretical studies, J. Phys. Chem. A 114 (2010) 9425–9439.
[47] W.K. Metcalfe, S.M. Burke, S.S. Ahmed, H.J. Curran, A hierarchical and comparative kinetic modeling study of C1 − C2 hydrocarbon and oxygenated fuels, Int. J. Chem. Kinet. 45 (2013) 638–675.
[48] Y. Zhang, H. El-Merhubi, B. Lefort, L. Le Moyne, H.J. Curran, A. Kéromnès, Probing the low-temperature chemistry of ethanol via the addition of dimethyl ether, Combust. Flame 190 (2018) 74–86.
[49] D. Nativel, P. Niegemann, J. Herzler, M. Fikri, C. Schulz, Ethanol ignition in a high-pressure shock tube: ignition delay time and high-repetition-rate imaging measurements, Proc. Combust. Inst. 38 (2021) 901–909.
[50] K.E. Noorani, B. Akih-Kumgeh, J.M. Bergthorson, Comparative high temperature shock tube ignition of C1−C4 primary alcohols, Energy Fuels 24 (2010) 5834–5843.
[51] A.R. Laich, E. Ninnemann, S. Neupane, R. Rahman, S. Barak, W.J. Pitz, S. S. Goldsborough, S.S. Vasu, High-pressure shock tube study of ethanol oxidation: ignition delay time and CO time-history measurements, Combust. Flame 212 (2020) 486–499.
[52] N. Leplat, P. Dagaut, C. Togbé, J. Vandooren, Numerical and experimental study of ethanol combustion and oxidation in laminar premixed flames and in jet-stirred reactor, Combust. Flame 158 (2011) 705–725.